

## Supporting Information

### Ultrasonically assisted conversion of uranium trioxide into uranium(VI) intrinsic colloids

Manon Cot-Auriol <sup>a</sup>, Matthieu Virost <sup>a</sup>, Cyril Micheau <sup>a</sup>, Xavier Le Goff <sup>a</sup>, Christophe Den Auwer<sup>c</sup>,  
Thomas Dumas <sup>b</sup>, Olivier Diat <sup>a</sup>, Philippe Moisy <sup>b</sup>, Sergey I. Nikitenko <sup>a</sup>

<sup>a</sup> ICSM, Univ Montpellier, CEA, CNRS, ENSCM, Marcoule, France.

<sup>b</sup> CEA, DES, ISEC, DMRC, Univ Montpellier, Marcoule, France.

<sup>c</sup> Université Côte d'Azur, CNRS, Institut de Chimie de Nice, Nice, France.

**Figure S1**

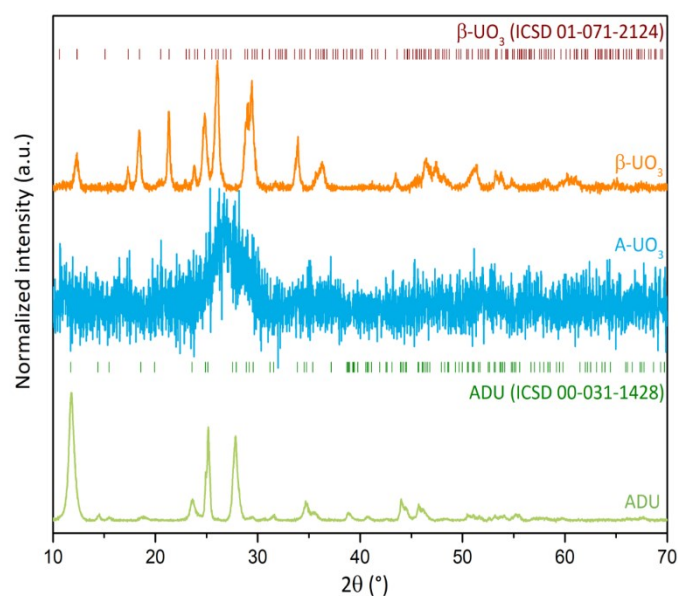


Fig. S1: Normalized PXRD diagrams (background corrected) acquired on ADU precursor (green), A- $\text{UO}_3$  powder (blue) and  $\beta$ - $\text{UO}_3$  powder (orange).

**Figure S2**

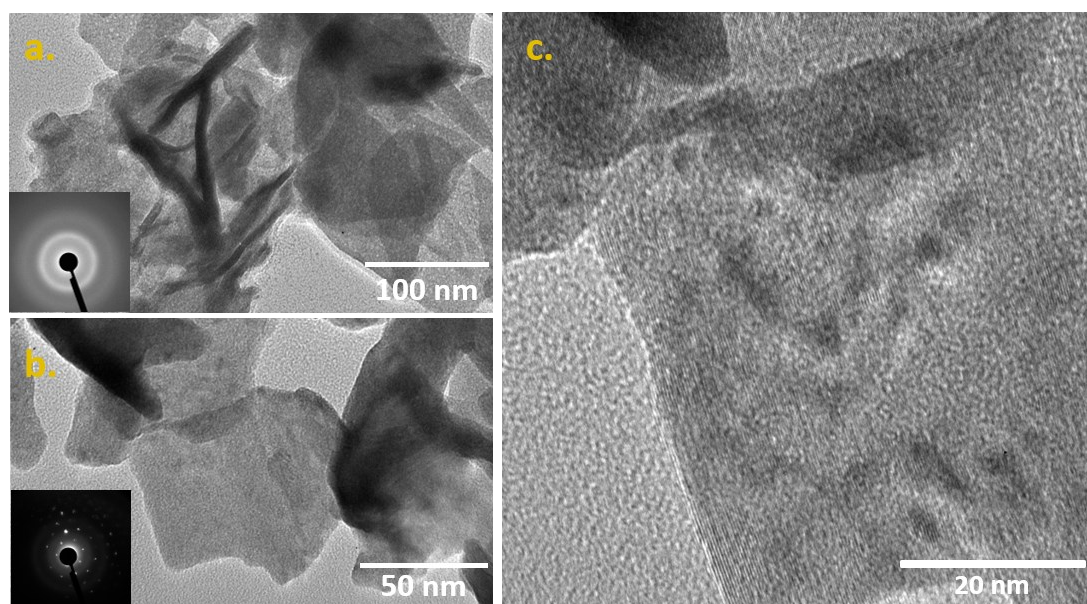


Fig. S2: HR-TEM analyses of U(VI) oxide powders obtained after calcination of the ADU precursor. Insets are the selected-area electron diffraction (SAED) patterns collected for each powder. (a) A- $\text{UO}_3$  powder, (b) - (c)  $\beta$ - $\text{UO}_3$  powder at different magnifications.

**Figure S3**

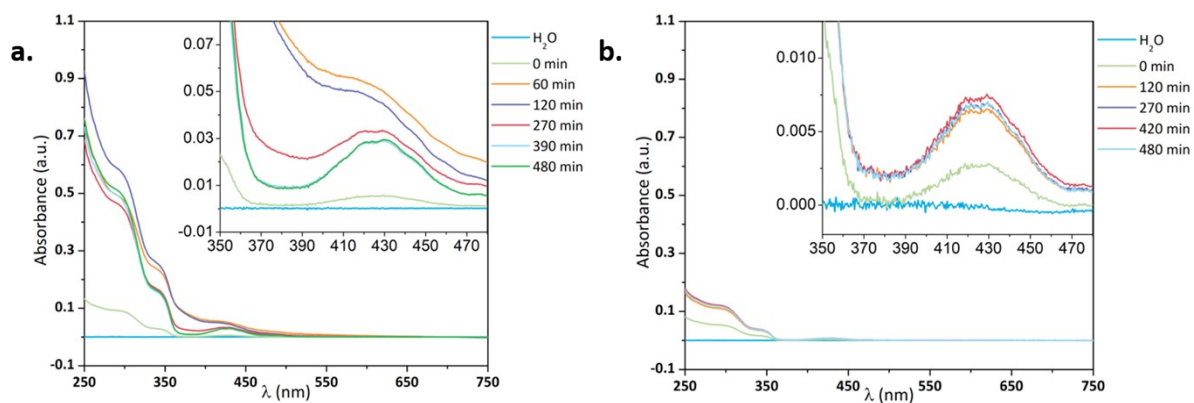


Fig. S3: UV-Vis absorption spectra observed during the treatment of  $\beta$ - $\text{UO}_3$  in pure water under (a) sonication at 20 kHz ultrasound (20 °C, Ar/(10%)CO, 0.35 W.mL<sup>-1</sup>) and (b) mechanical stirring (silent conditions).

**Figure S4**

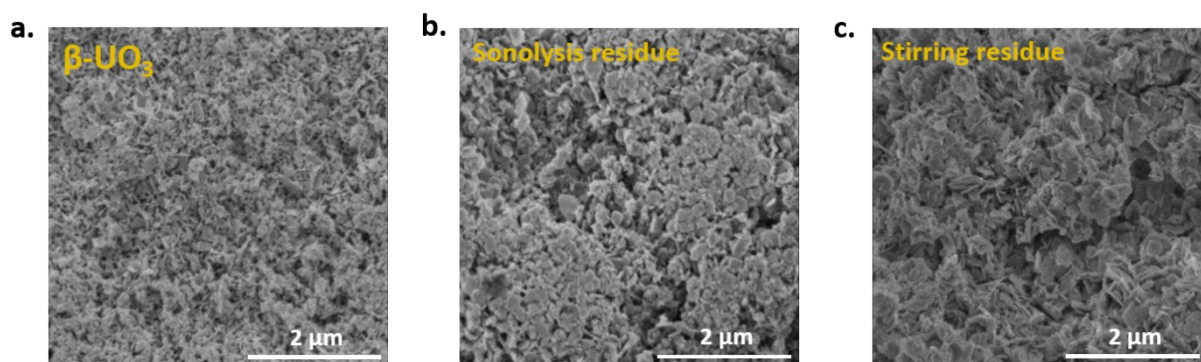


Fig. S4: SEM images of  $\beta\text{-UO}_3$  (a) before treatment, (b) after sonication (20 kHz, 20 °C, Ar/(10%)CO, 0.35 W.mL<sup>-1</sup>) and (c) after mechanical stirring in silent conditions.

**Figure S5**

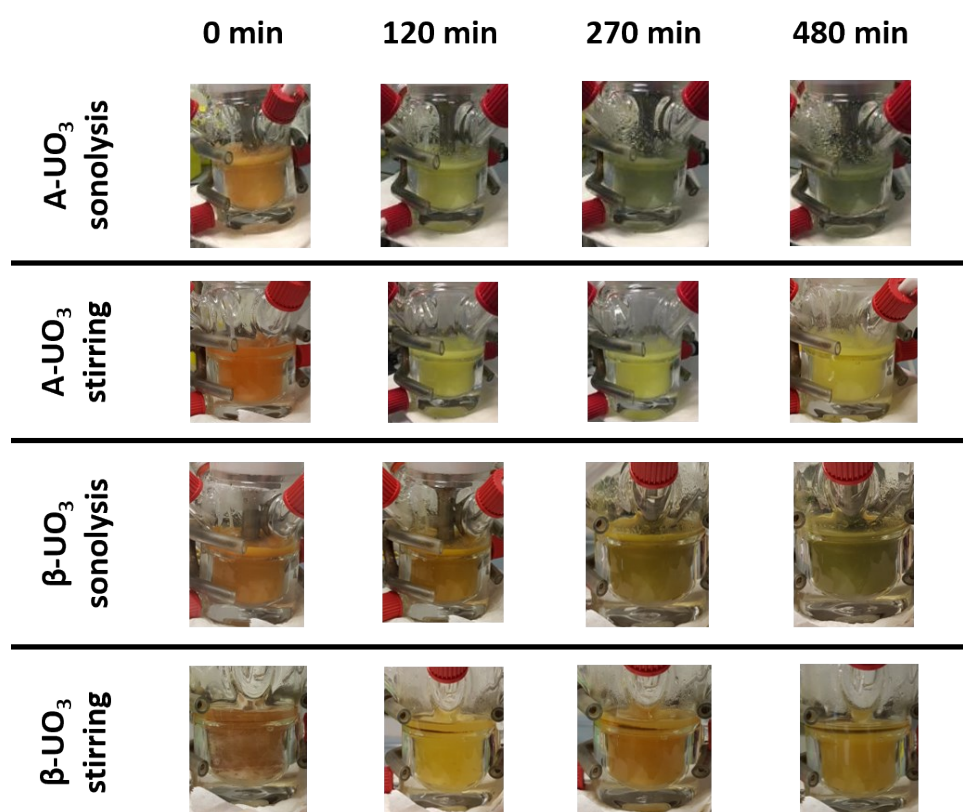


Fig. S5: Photos of the glass reactor during  $\text{UO}_3$  powder treatments by sonication at 20 kHz ultrasound (20 °C, Ar/(10%)CO, 0.35 W.mL<sup>-1</sup>) and mechanical stirring (silent conditions).

**Figure S6**

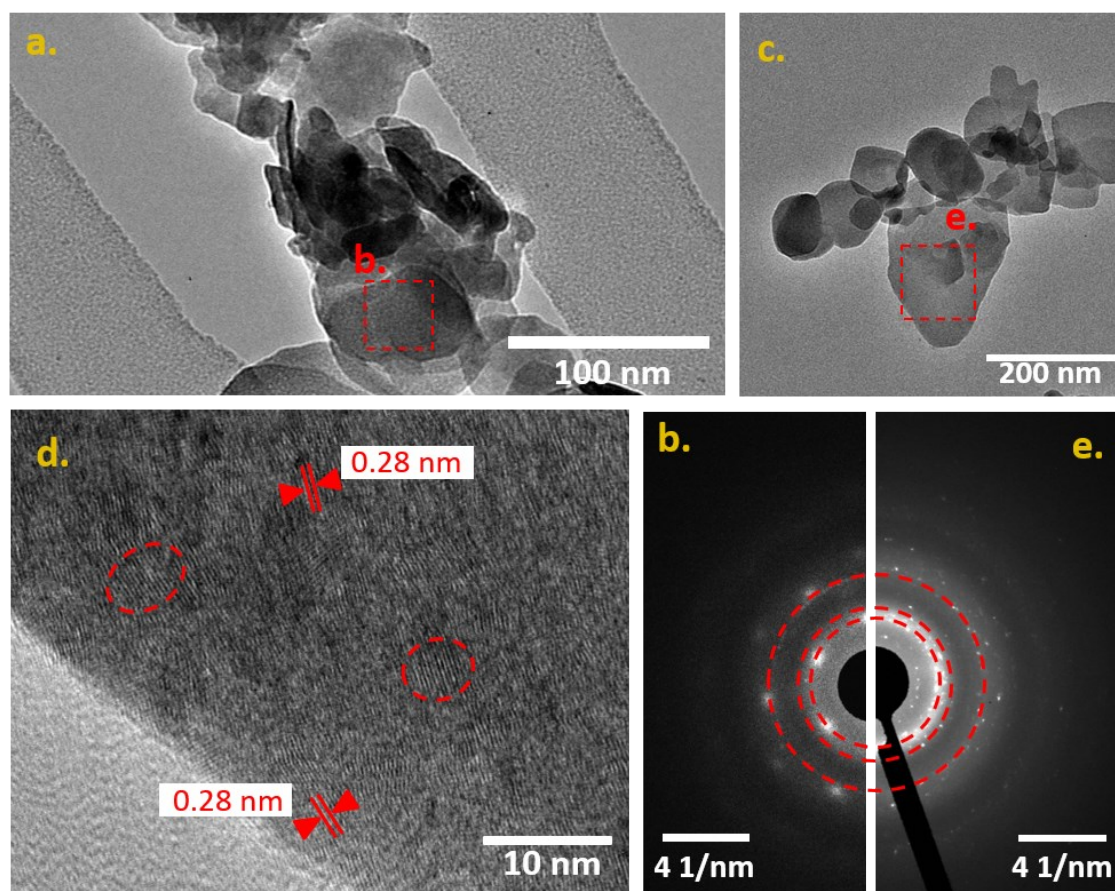


Fig. S6: HR-TEM analyses of the neofomed solids obtained after treatment of  $\beta$ - $\text{UO}_3$  powder. Dashed squares represent the selected areas corresponding to an analysis by electron diffraction (SAED). Dashed circles denote individual nanoparticles. (a) Sonolysis residue, (b) SAED pattern of an aggregate formed during sonolysis, (c) - (d) stirring residue at different magnifications and (e) SAED pattern of a polycrystalline nanoparticle aggregate formed during mechanical stirring. In panels (b) and (e), dashed circles correspond to  $\text{UO}_2$  diffraction rings.<sup>1</sup>

**Table S1**

Table S1:  $d_n$  spacing values (for  $1 \leq n \leq 4$ ) of theoretical crystals ( $\text{UO}_2$ , schoepite, *meta*-schoepite), neoformed solids obtained after  $\text{UO}_3$  treatments and A- $\text{UO}_3$  sonolysis supernatant.<sup>1</sup> For schoepite and *meta*-schoepite,  $d_n$  values are calculated from corresponding ICSD patterns (ICSD 00-013-0241 and ICSD 01-070-4765, respectively). For experimental samples,  $d_n$  values are measured on HR-TEM SAED patterns. The error is estimated equal to  $\pm 0.2 \text{ \AA}$ .

	$\text{UO}_2$	$d_n$ ( $\text{\AA}$ )	3.15	2.73	1.93	1.65
	Schoepite	$d_n$ ( $\text{\AA}$ )	7.21	4.38	3.59	3.55
	<i>Meta</i> -schoepite	$d_n$ ( $\text{\AA}$ )	8.48	8.17	7.19	6.32
HR-TEM	A- $\text{UO}_3$ sonolysis residue	$d_n$ ( $\text{\AA}$ )	3.41	2.95	2.09	1.78
		$d_1/d_n$ ( $\text{\AA}$ )	-	1.16	1.63	1.92
	A- $\text{UO}_3$ sonolysis supernatant	$d_n$ ( $\text{\AA}$ )	3.14	2.74	1.89	1.66
		$d_1/d_n$ ( $\text{\AA}$ )	-	1.15	1.66	1.90
	A- $\text{UO}_3$ stirring residue	$d_n$ ( $\text{\AA}$ )	3.33	2.90	2.06	1.75
		$d_1/d_n$ ( $\text{\AA}$ )	-	1.15	1.62	1.91
	$\beta$ - $\text{UO}_3$ sonolysis residue	$d_n$ ( $\text{\AA}$ )	3.36	2.90	2.03	1.74
		$d_1/d_n$ ( $\text{\AA}$ )	-	1.16	1.66	1.93
	$\beta$ - $\text{UO}_3$ stirring residue	$d_n$ ( $\text{\AA}$ )	3.31	2.90	2.00	1.71
		$d_1/d_n$ ( $\text{\AA}$ )	-	1.14	1.65	1.94

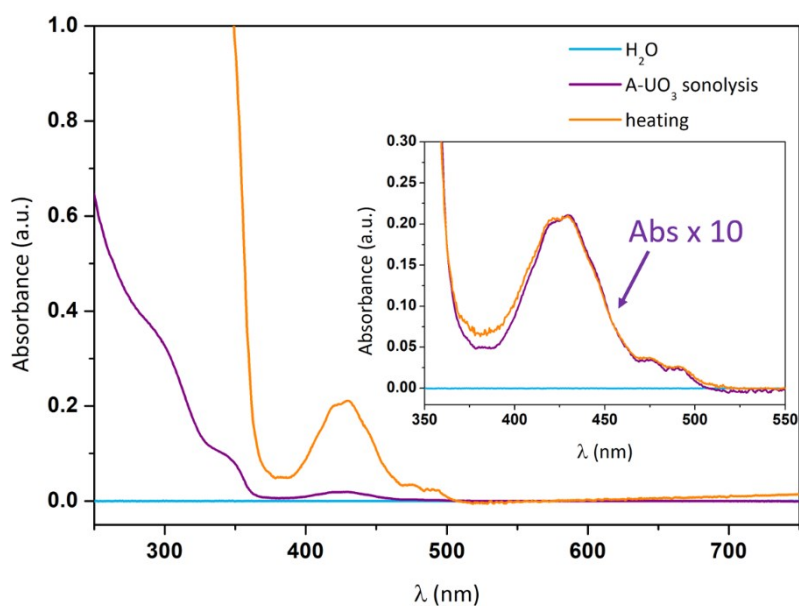
**Figure S7**

Fig. S7: UV-Vis absorption spectra of supernatant obtained after sonolysis of A- $\text{UO}_3$  in pure water. The spectra are measured before and after concentration by heating. The inset shows the initial spectrum (purple line) multiplied by 10 for comparison.

**Figure S8**

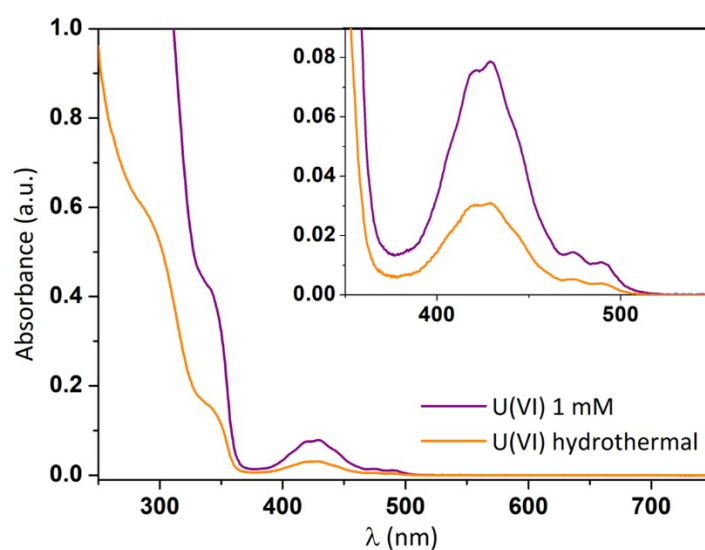


Fig. S8: UV-Vis absorption spectra of a 1 mM aqueous U(VI) solution before (purple line) and after (orange line) hydrothermal treatment (200 °C, 3 h).

**Figure S9**

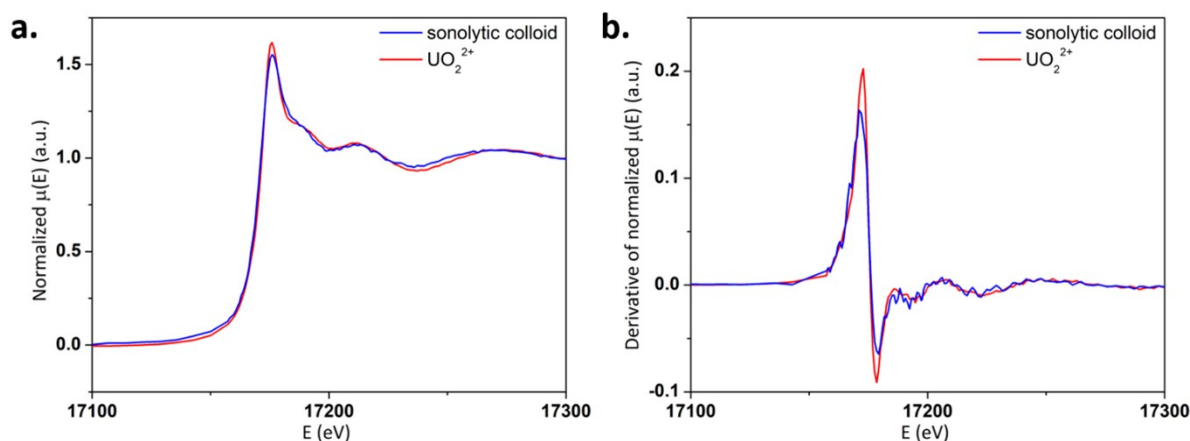


Fig. S9: (a) U  $L_{III}$  XANES experimental spectrum acquired on sonolytic colloids of U(VI) obtained after A- $UO_3$  treatment (blue line). In addition,  $UO_2^{2+}$  (aquo form in pure water) XANES spectrum is provided for comparison (red line)<sup>2</sup>. (b) The corresponding derivatives of XANES spectra for sonolytic colloids (blue line) and  $UO_2^{2+}$  (red line).

**Figure S10**

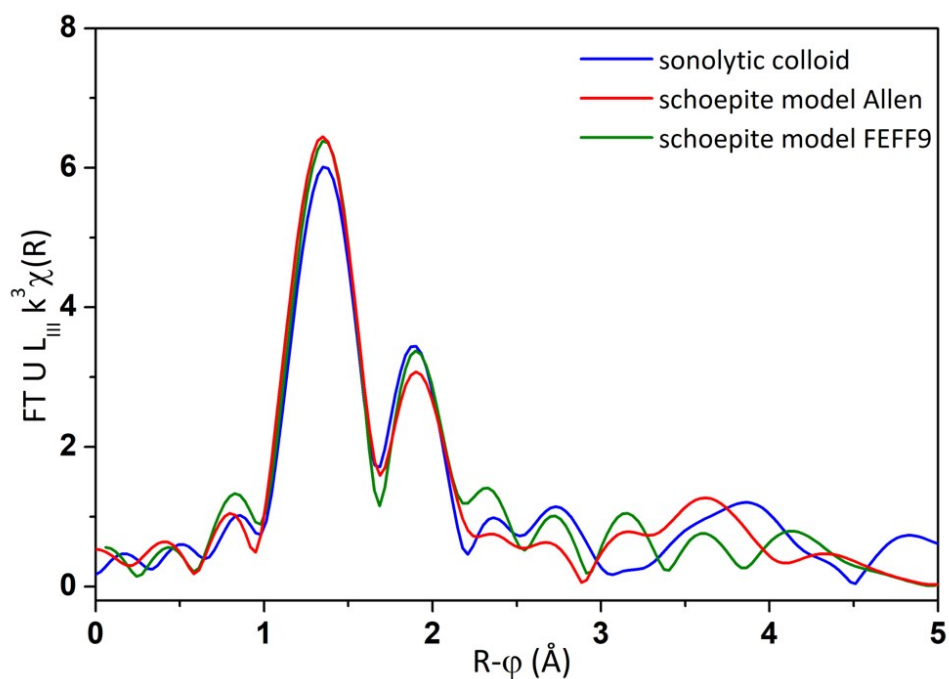


Fig. S10: Fourier transforms (FT) of the  $k^3$ -weighted 2.5-11.2  $\text{\AA}^{-1}$  range for the sonolytic colloids obtained after A- $\text{UO}_3$  treatment (blue line) compared to the schoepite model (green line) obtained with FEFF9 full scattering calculation and the schoepite model (red line) reconstructed from Allen's fit parameters.<sup>3</sup>

**Figure S11**

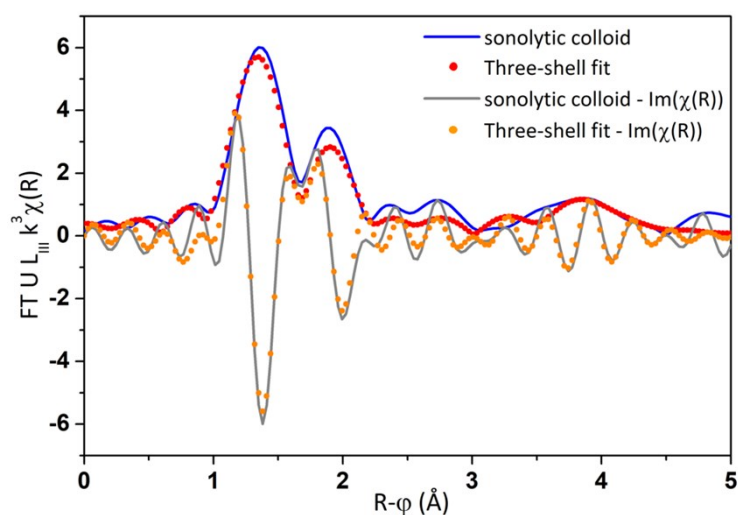


Fig. S11: Fourier transforms (FT) of the  $k^3$ -weighted 2.5-11.2  $\text{\AA}^{-1}$  range for sonolytic colloids obtained after A- $\text{UO}_3$  treatment (blue line) and the corresponding fit using a three-shell model (red points). In addition, the imaginary parts are plot (in grey line and orange points, respectively).

## **Table S2**

Table S2: Model and parameters considered for the F-test on EXAFS fits of U(VI) colloids sample for the four-shell fit with/without the U-U shell. R is equal to the square root of the IFFEFIT parameter R-factor. n is the number of free parameters used in the corresponding fit and m the number of independent data points.

<b>Shells</b>	<b>R</b>	<b>n</b>	<b>k range (<math>\text{\AA}^{-1}</math>)</b>	<b>R range (<math>\text{\AA}</math>)</b>	<b>m*</b>	<b>F<sup>4</sup></b>
O <sub>yl</sub> , O <sub>eq1</sub> , O <sub>eq2</sub> , U	0.221	10	2.5-11.2	1.1-5	23.6	4.2
O <sub>yl</sub> , O <sub>eq1</sub> , O <sub>eq2</sub>	0.307	7				

\*calculated according to the Stern's rule<sup>5</sup>

## **References**

- 1 T. M. Nenoff, B. W. Jacobs, D. B. Robinson, P. P. Provencio, J. Huang, S. Ferreira and D. J. Hanson, *Chem. Mater.*, 2011, **23**, 5185–5190.
- 2 M. Duvail, T. Dumas, A. Paquet, A. Coste, L. Berthon and P. Guilbaud, *Phys. Chem. Chem. Phys.*, 2019, **21**, 7894–7906.
- 3 P. G. Allen, D. K. Shuh, J. J. Bucher, N. M. Edelstein, C. E. A. Palmer, R. J. Silva, S. N. Nguyen, L. N. Marquez and E. A. Hudson, *Radiochim. Acta*, 1996, **75**, 1–23.
- 4 L. Downward, C. H. Booth, W. W. Lukens and F. Bridges, in *AIP Conference Proceedings*, AIP, Stanford, California (USA), 2007, vol. 882, pp. 129–131.
- 5 E. A. Stern, *Phys. Rev. B*, 1993, **48**, 9825–9827.